

Experimental and Modeling Study of Continuous Catalytic Transesterification to Biodiesel in a Bench-Scale Fixed-Bed Reactor

Yang Xiao, Lijing Gao, Guomin Xiao,* Baosong Fu, and Lei Niu

School of Chemistry and Chemical Engineering, Southeast University, Nanjing 211189, People's Republic of China

ABSTRACT: A 500 h endurance test of continuous catalytic transesterification to biodiesel was conducted in a bench-scale fixed-bed reactor. A designed cylinder shape of KF/Ca–Mg–Al hydrotalcite catalyst was stable through the test with high catalytic activity and mechanical strength, converting palm oil to biodiesel with a conversion of more than 95%. Conditions effects on transesterification under relative high pressure (1.0 MPa) were investigated and a one-dimensional heterogeneous model of a fixed-bed reactor was developed to describe the reaction-mass transfer behaviors of continuous catalytic transesterification in a bench-scale fixed-bed reactor. With the given reactor size, optimum conditions were proposed as a LHSV (liquid hourly space velocity) of 0.76–0.25 h⁻¹, molar ratio of methanol-to-oil of 9.16–13.7, and temperature of 338–347 K.

1. INTRODUCTION

As the energy crisis and environmental pollution become increasingly problematic, and more attentions are paid to low carbon emissions and energy consumption issues, the use of fossil fuels is considered to decrease in energy fields all over the world. Alternative energy and resources, renewable, economic, and environmentally friendly, are therefore regarded as a top priority for both developed and developing nations. Biodiesel, which is synthesized by transesterification of vegetable oil, waste cooking oil, or animal fat with methanol, ethanol, or other lower alcohols, is one of these resources.^{1,2}

Transesterification in most biodiesel production is a catalytic reaction process either in a batch or continuous reactor. Catalysts are classified as homogeneous and heterogeneous ones. Homogeneous ones including sodium hydroxide, sodium methoxide, potassium hydroxide, potassium methoxide, sodium amide, and sulfuric acid, which have been used in a batch reactor, are more efficient; however, they bring problems of waste treatment and equipment corrosion. Much research and development is focused on heterogeneous catalysts used in a fixed bed reactor, such as alkaline earth metal oxides and various alkaline metal compounds supported on alumina or zeolites, which can catalyze transesterification of vegetable oil and alcohols efficiently as well.^{3,4} Unlike in the case of homogeneous catalysis, separating catalysts from the reactive mixture is much easier in a heterogeneous catalytic process and catalysts can be recycled.^{5,6} However, the heterogeneous catalysts may tend to lose their catalytic activity after long-term use because of impurity toxicity, active component leaching, and glycerol inhibition.

There is also literature that reports biodiesel production with a noncatalytic process. A supercritical or subcritical technique is employed to overcome catalyst deactivation when heterogeneous catalysts are used. The key operating parameters are pressure, temperature, and molar ratio of methanol-to-oil. To achieve high conversion of biodiesel, high pressure (19–45 MPa), high temperature (593–623 K), and a high molar ratio of methanol-to-oil (40:1–42:1) have been used in the literatures.^{7,8} Under such conditions, not only an expensive

reactor but also a sophisticated operation is required, which leads to a larger energy consumption.⁹

For these reasons, the combination of heterogeneous catalysis and supercritical or subcritical technology appeared. Khanh et al.¹⁰ investigated effects of reaction conditions on the transesterification of vegetable oil and methanol in a fixed-bed reactor under high pressure and elevated temperature catalyzed by zinc aluminate. Unfortunately low conversion 5–70% was reported which may have resulted from low activity of the catalyst. Clayton et al.¹¹ developed a novel continuous fixed-bed reactor process for the production of biodiesel using a metal oxide-based catalyst. They claimed the catalysts, chemically, thermally, and mechanically stable, could be operated under subcritical alcohol conditions for continuous long-term biodiesel fuel production without loss of catalytic activity over extended use. But the temperature (573–723 K) and pressure (17.2 MPa) set a high threshold for the equipments, and more energy would be consumed when per ton of biodiesel was produced. Sandra et al.¹² analyzed several different schemes theoretically for industrial FAME (fatty acid methyl ester) production at higher pressure and temperature, and pointed out that energy consumption mainly depended on degree of conversion of triglycerides, while a further significant decrease of energy consumption might be obtained at subcritical conditions with the use of an appropriate catalyst. Chen Jie et al.¹³ developed a pseudo-first-order kinetic model of continuous transesterification catalyzed by KOH in a static mixing tubular reactor. Ke Zhonglu et al.¹⁴ reported that under continuous catalytic transesterification for 28.7 h using regenerating resin, the catalytic activity did not decline.

In our previous works, KF/Ca–Mg–Al hydrotalcite was reported as a very high activity catalyst for conversion in transesterification of vegetable oil and methanol.¹⁵ In this study,

Special Issue: Alternative Energy Systems

Received: October 9, 2011

Revised: February 20, 2012

Accepted: March 5, 2012

Published: March 5, 2012

a 500 h continuous catalytic operation was conducted to test the stability of the designed cylinder shape catalyst. Conditions effects of transesterification in a bench-scale fixed-bed reactor were also investigated under relative high pressure, and a one-dimensional heterogeneous model was developed to describe behaviors of catalysis and mass transfer in the bench-scale fixed-bed reactor.

2. EXPERIMENTAL SECTION

2.1. Chemicals. Palm oil was purchased from the Nanjing Runtai market. CH_3OH was purchased from Nanjing Chemical Reagent Co., Ltd. $(\text{CH}_3)_2\text{CH-O-CH}(\text{CH}_3)_2$ was purchased from Shanghai Lingfeng Chemical Reagent Co., Ltd. $\text{KF}\cdot 2\text{H}_2\text{O}$, $\text{Ca}(\text{NO}_3)_2\cdot 4\text{H}_2\text{O}$, $\text{Mg}(\text{NO}_3)_2\cdot 6\text{H}_2\text{O}$, $\text{Al}(\text{NO}_3)_3\cdot 9\text{H}_2\text{O}$, NaOH , and Na_2CO_3 were purchased from Guangdong Guanghua Chemical Factory Co., Ltd.

2.2. Experimental Procedure and Apparatus. The $\text{KF}/\text{Ca-Mg-Al}$ hydrotalcite catalyst powder was prepared by the procedure described in our previous work.¹⁵ Briefly, the Ca-Mg-Al hydroxides were prepared by the coprecipitation method. Solution A (2000 mL) contained a certain amount of $\text{Ca}(\text{NO}_3)_2\cdot 4\text{H}_2\text{O}$ (1.5 mol), $\text{Mg}(\text{NO}_3)_2\cdot 6\text{H}_2\text{O}$ (1.5 mol), and $\text{Al}(\text{NO}_3)_3\cdot 9\text{H}_2\text{O}$ (1.0 mol), while solution B (2000 mL) contained NaOH (4.0 mol) and Na_2CO_3 (1.0 mol). Both solutions were synchronously dropped into 1000 mL of water at 338 K slowly, accompanied with vigorous mechanical stirring, while the pH was maintained between 10 and 11. The resulting mixture was held at 338 K while continuing to stir vigorously for 48 h and then filtered and washed with water until the pH value of the filtrate was near 7. The precipitate was dried at 373–398 K overnight and calcined at 723 K for 5 h. The calcined powder was ground with $\text{KF}\cdot 2\text{H}_2\text{O}$, with the mass ratio of 100% (wt/wt calcined powder), while dropping some water. Then, the paste was dried at 338 K overnight. Catalyst was shaped by double screw extrusion machine (HYNJ-0.25 L). After drying and calcination, the 1 mm diameter cylinder catalyst was cut into 2 mm length.

The nitrogen adsorption isotherms were measured at 77 K on a Micromeritics ASAP 2020 apparatus. Before measurements, the samples were degassed at 623 K for 5 h in vacuum. The specific surface areas of the samples were calculated using the BET isothermal equation and the pore volume was evaluated by the t -plot method.

Experiments were conducted in the experimental system depicted in Figure 1. The length of bench-scale fixed-bed reactor was 800 mm, and the height of catalyst packed in the reactor was 600 mm in the experiments. The inner diameter of the reactor was 50 mm. The cylinder catalysts were packed in the middle of the reactor along with quartz sand and rock wool.

Two plunger piston pumps providing a top discharge pressure of 10.0 MPa and capable of delivering a max flow of 60 mL/min were applied. Methanol and mixture of palm oil and isopropyl ether, heated to specific temperature respectively, were pumped through a static mixer and then into the reactor. Temperature of the reactor was detected by several thermocouples and controlled by a programmable logic controller (PLC) system with a precision of 0.5 K. The pressure of the system was maintained through the use of backpressure regulators of Tescom (Elk River, MN). After the transesterification, products were collected after a water-cooled trap. When all the operation parameters were stable, productions were analyzed offline by a gas chromatograph (Ouhua GC 9160) equipped with a DB-5Ht capillary column

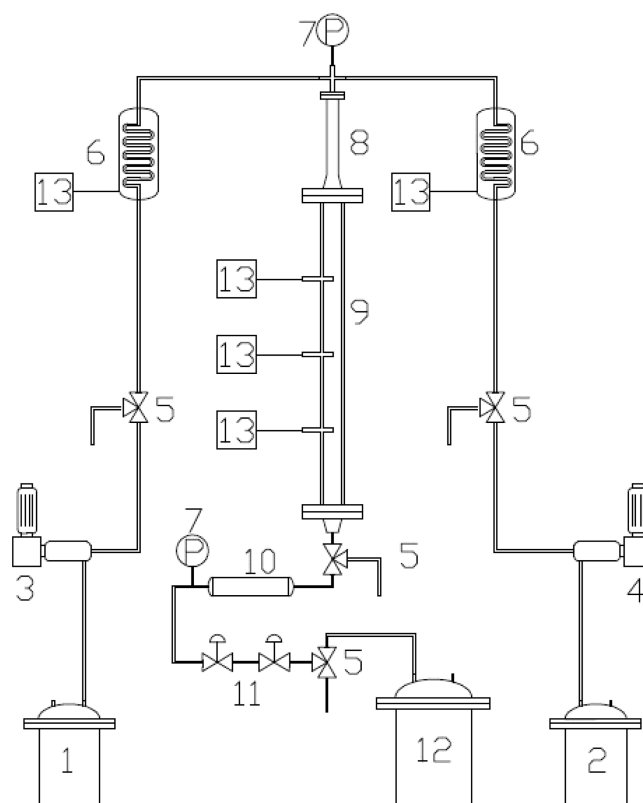


Figure 1. Overall experimental system schematic.

(15 m × 0.25 mm × 0.25 mm) via a flame ionization detector (FID).

3. RESULTS AND DISCUSSION

3.1. Catalyst Endurance Test. Some parameters of cylinder catalysts and the reactor were listed in Table 1. (All the symbols used in this paper were defined in the Nomenclature section.)

The relative high temperature (363 K), pressure (1.0 MPa), molar ratio of methanol-to-oil ($m = 22.73$), and relative slow LHSV (liquid hourly space velocity) (0.25 h^{-1}) were adopted in the catalyst endurance test to achieve close to 100% conversion.

Table 1. Parameters of Cylinder Catalysts and Reactor

parameters	units	values
d_t	m	40×10^{-3}
L	m	600×10^{-3}
ϵ		0.5192
d_p	m	1.2×10^{-3}
a	$\text{m}^2\cdot\text{m}^{-3}$	3.65×10^6
S_e	$\text{m}^2\cdot\text{m}^{-3}$	5.00×10^3
V_g	$\text{m}^3\cdot\text{kg}^{-3}$	3.09×10^{-5}
θ		0.0713
δ		4.1
ρ_b	$\text{kg}\cdot\text{m}^{-3}$	1109.0
ρ_p	$\text{kg}\cdot\text{m}^{-3}$	2306.4
ρ_t	$\text{kg}\cdot\text{m}^{-3}$	2483.5

Values of V_g , θ , a , ρ_b , ρ_p , ρ_t were calculated based on nitrogen adsorption isotherms data. S_e and ϵ were calculated according

Figure 1 showed that the cylinder catalyst packed in a fixed bed maintained greater than 95% conversion efficiency over 500 h of continuous operation without significant loss in conversion and mechanical strength. This result was very important in that it demonstrated the catalytic systems studied in this paper could be operated for extended use because of their chemical, thermal, and mechanical stability. It also meant that the catalyst could be used for a long period without significant deviation, and the results were steady under the stable operation parameters.

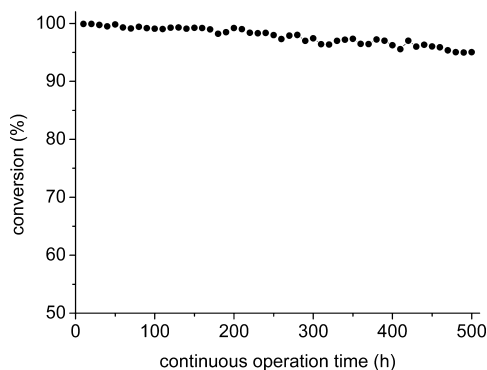


Figure 2. Catalyst endurance test ($T = 363$ K, $p = 1.0$ MPa, $m = 22.73$, LHSV = 0.25 h $^{-1}$).

3.2. Development of Fixed-Bed Reactor Model.

3.2.1. Model Assumptions. The mathematical model for the fixed-bed reactor was based on the following assumptions: (1) the feed current to reactor was plug flow ($dt/dp > 10$, $L/dp > 100$);¹⁷ (2) the reactor was operated under steady state conditions; (3) the reactor was in isobaric and isothermal operation; (4) densities and viscosities of each component from NIST Standard Database were fitted into functions of temperature, and a weighted-to-weighted model was used to estimate related properties of the liquid mixture.

3.2.2. Mathematical Model. To reveal the mechanism of the heterogeneous catalysis, an intrinsic kinetic model was developed on the basis of the Eley–Rideal mechanism in our previous paper.¹⁸ In the model, the transesterification occurred between methanol adsorbed on solid base active sites and glyceride from the liquid phase, and the surface reaction of triglyceride with adsorbed methanol was assumed to be rate-determining. The intrinsic kinetic model was expressed as follows:

$$r = \frac{k \left(C_{b1}C_{b2} - \frac{1}{K} \frac{C_{b3}^3 C_{b4}}{C_{b2}^2} \right)}{1 + K_2 C_{b2} + K_4 C_{b4}} \quad (1)$$

The values of parameters k , K , K_2 , K_4 also came from ref 18.

When external diffusion effects were included, the expression was revised to

$$r_e = \frac{k \left(C_{s1}C_{s2} - \frac{1}{K} \frac{C_{s3}^3 C_{s4}}{C_{s2}^2} \right)}{1 + K_2 C_{s2} + K_4 C_{s4}} \quad (2)$$

where C_{si} was concentration of component i at the external surface of catalyst.

The external diffusion effectiveness factor η_e was defined as followed:

$$\eta_e = \frac{r_e}{r} \quad (3)$$

The external diffusion effectiveness factor could reflect how the difference of reactant concentration in bulk fluid and at the external surface of catalyst influenced the overall reaction rate.

When the internal diffusion effects were included, the expression was modified to¹⁹

$$r_{ei} = \eta r_e = \eta = \frac{k \left(C_{s1}C_{s2} - \frac{1}{K} \frac{C_{s3}^3 C_{s4}}{C_{s2}^2} \right)}{1 + K_2 C_{s2} + K_4 C_{s4}} \quad (4)$$

where η is the internal diffusion effectiveness factor. There was a theoretical relationship between the effectiveness factor η and the well-known Thiele modulus Φ .²⁰

$$\eta = \frac{1}{\Phi} \left[\frac{1}{\tanh(3\Phi)} - \frac{1}{3\Phi} \right] \quad (5)$$

where the Thiele modulus was a function of the catalyst size, reaction rate including external diffusion, concentration in bulk fluid of oil and effective diffusivity.²¹

$$\Phi = \frac{V_p}{S_p} \sqrt{\frac{r_{se}}{C_{b10} D_{eff}}} \quad (6)$$

The diffusion coefficients were estimated by the Wike and Chang equation:²²

$$D_{AB} = \frac{1.17 \times 10^{-13} (\xi_B M_B)^{0.5} T}{V_A^{0.6} 100 \mu_1} \quad (7)$$

1.0 was the recommended value for the association factor ξ_B when isopropyl ether was used as a solvent, and effective diffusivity was estimated:

$$D_{eff} = \frac{D_1}{\delta} \theta \quad (8)$$

Table 2. D and k_{LS} Values of Each Component at 338 K

components	palm oil	methanol	biodiesel	glycerol
D (m 2 ·s $^{-1}$)	2.26×10^{-10}	3.00×10^{-10}	2.12×10^{-10}	3.33×10^{-10}
k_{LS} (m·s $^{-1}$)	3.7×10^{-7}	5.00×10^{-7}	3.53×10^{-7}	5.54×10^{-7}

According to the steady state conditions, mass transfer rates were equal to reaction rate:

$$\begin{aligned}\eta\rho_b r_e &= k_{LS1}S_e(C_{b1} - C_{s1}) \\ &= \frac{1}{3}k_{LS2}S_e(C_{b2} - C_{s2}) \\ &= \frac{1}{3}k_{LS3}S_e(C_{s3} - C_{b3}) \\ &= k_{LS4}S_e(C_{s4} - C_{b4})\end{aligned}\quad (9)$$

Mass transfer coefficients at the liquid–solid interface were calculated using Calderbank and Moo-Young correlation:²³

$$k_{LS}d_p D^{-1} = 2 + 0.31D^{5/3}\left(\frac{\rho_s - \rho_l}{\mu_l}\right)^{1/3}\quad (10)$$

D and k_{LS} values of each component at 338 K are listed in Table 2.

Table 2 showed that D and k_{LS} values of palm oil were lower than that of methanol and it indicated that the mass transfer of oil from bulk fluid to catalyst external surface was a major factor in the reaction-mass transfer process.

Numerical computing methods were employed to solve simultaneous eqs 2–10, and the macroscopic kinetic model including mass transfer effects was obtained.

3.3. External and Internal Diffusion Effects. Calculation of the model showed a high external diffusion effectiveness factor value ($\eta_e = 0.94$ – 0.99) while it provided a low internal diffusion effectiveness factor ($\eta = 0.04$ – 0.08).

When relative high pressure (1.0 MPa) and isopropyl ether as cosolvent were used in the system,^{24–26} the liquid–solid phase reaction between 298 and 348 K was ensured, and the two–phase system enhanced the mass transfer rate by a wider margin, comparing with gas–liquid–solid or liquid–liquid–solid three-phase systems, which may be an important reason for a high external diffusion effectiveness factor. Therefore the external diffusion mass transfer resistance was so little that external diffusion effects were negligible.

The high mechanical strength cylinder catalyst showed a low specific pore volume and a corresponding low porosity ($\theta = 0.0713$). It resulted in low effective diffusivity obstructing reactants from entering into catalyst pore. As calculation demonstrated, a low internal diffusion effectiveness factor meant the total reaction rate was dominated by an intrapore diffusion process so that low LHSV was needed to obtain high conversion, which was also proved by our LHSV effects experiments.

3.4. One-Dimensional Heterogeneous Model of a Fixed Bed Reactor. Equation 11 was used to calculate the void fraction:²⁷

$$\varepsilon = 0.38 + 0.073 \left[1 + \frac{\left(\frac{d_t}{d_p} - 2 \right)^2}{\left(\frac{d_t}{d_p} \right)^2} \right]\quad (11)$$

The void fraction was 0.5192 and used in eq 12 to estimate pressure drop of the fixed bed reactor.²⁸

$$\frac{\Delta p}{L} = 150 \frac{(1 - \varepsilon)^2}{\varepsilon^3} \frac{\mu_l u_l}{d_s^2} + 1.75 \frac{\rho_l u_l^2}{d_s} \frac{(1 - \varepsilon)^2}{\varepsilon^3}\quad (12)$$

The pressure drop was 152.44 Pa, and it was insignificant to the operation pressure, meaning the isobaric assumption was reasonable.

The one-dimensional heterogeneous model was employed to describe reaction–mass transfer behaviors of transesterification in the bench-scale fixed-bed reactor. The differential equation of the fixed-bed reactor including mass transfer was expressed as²⁸

$$-u_l \frac{dC_l}{dL} = k_{LS1}S_e(C_{b1} - C_{s1})\quad (13)$$

Equation 13 was simplified to

$$\frac{dx}{dL} = \frac{\eta_e \rho_b}{u_l C_{b10}}\quad (14)$$

The boundary conditions were $L = 0$, $x = 0$. Numerical computing methods were employed to solve the simultaneous eqs 2–12 and ordinary differential eq 14, and then HLSV, temperature, and molar ratio of methanol-to-oil effects on transesterification conversion were illustrated.

3.4.1. HLSV Effects on Transesterification Conversion. From Figure 3 we could see that model calculations agreed well

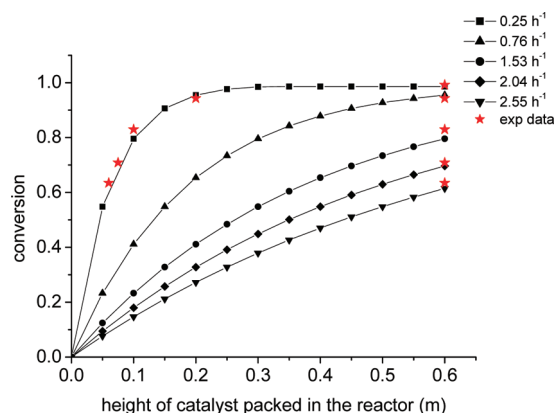


Figure 3. Experimental data and model calculations of HLSV effects on transesterification conversion at $T = 343$ K, $p = 1.0$ MP, and $m = 22.73$.

with experimental value and conclude that low HLSV (e.g., 0.25– 0.76 h^{-1}) was necessary to achieve more than 90% conversion. It could be explained by the very low internal diffusion effectiveness factor which made the intrapore diffusion process need more residence time of reactants. The LHSV experiments also proved that the differential model and numerical integral method were exact and that the experimental project of measuring conversion at the outlet of the fixed-bed reactor was reasonable.

3.4.2. Molar Ratio of Methanol-to-Oil Effects on Transesterification Conversion. From Figure 4 we could see when the molar ratio of the methanol-to-oil increased to 13.7, conversion got close to 100%, which meant that a higher molar ratio was unnecessary to improve conversion under the conditions of $\text{LHSV} = 0.25 \text{ h}^{-1}$ and $T = 338$ K. But with a

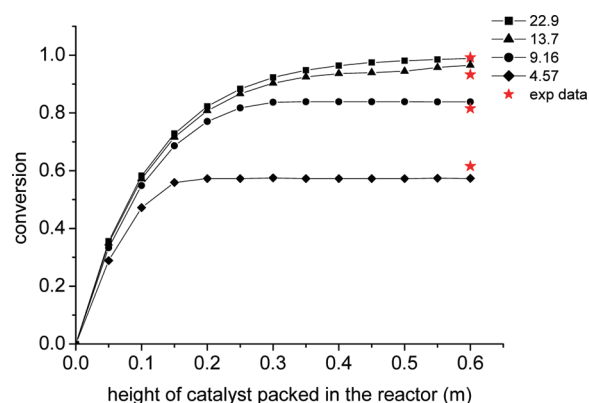


Figure 4. Experimental data and model calculations of molar ratio of methanol-to-oil effects on transesterification conversion at LHSV = 0.25 h^{-1} and $T = 338 \text{ K}$, $p = 1.0 \text{ MPa}$.

molar ratio less than 9.16 in Figure 5, conversion only reached about 80%. It can be explained by the fact that trans-

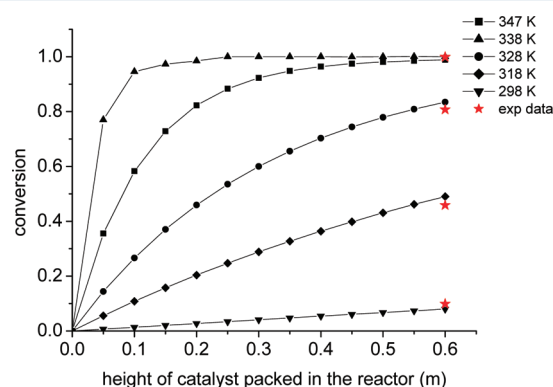


Figure 5. Experimental data and model calculations of temperature effects on transesterification conversion at LHSV = 0.25 h^{-1} , $p = 1.0 \text{ MPa}$ and $m = 22.73$.

esterification was an equilibrium reaction and a relative high molar ratio of methanol-to-oil was needed to obtain a greater equilibrium constant.

3.4.3. Temperature Effects on Transesterification Conversion. From Figure 5 we could see that model calculations agreed well with experimental value. Temperature impacted on conversion of transesterification dramatically. When temperature was higher than 338 K, the conversion of transesterification reached 95% rapidly through the catalyst bed. In contrast, when temperature was lower than 328 K, conversion could not come up to a satisfactory value. Temperature had a tremendous impact on conversion as a result of affecting not only density, viscosity, diffusion coefficient, effective diffusivity, mass transfer coefficient of each component or liquid mixture, but also adsorption equilibrium constant, rate constant, and reaction equilibrium constant of transesterification. All the factors above had been taken into account in our one-dimensional heterogeneous model of a fixed-bed reactor. As a consequence, temperature was the most significant aspect in the continuous transesterification system.^{18,29}

According to experiments and the one-dimensional heterogeneous model calculation, optimum conditions would be obtained in different scale reactors, and some optimum conditions were proposed in our bench scale reactor: LHSV

of $0.76\text{--}0.25 \text{ h}^{-1}$, molar ratio of methanol-to-oil of $9.16\text{--}13.7$, and temperature of $338\text{--}347 \text{ K}$.

4. CONCLUSIONS

A designed cylinder shape of KF/hydrotalcite catalyst was applied in fixed-bed reactor to catalyze palm oil to FAME by transesterification. With high catalytic activity and mechanical strength, the prepared catalyst maintained greater than 95% FAME conversion through 500 h of continuous operation without significant deactivation and mass loss.

A one-dimensional heterogeneous model of a fixed-bed reactor was developed to describe mass transfer-reaction behaviors of a continuous catalytic transesterification process, and the values predicted by the model at varied reaction parameters were highly consistent with that obtained in experiment. With the given reactor size, optimum conditions were proposed as LHSV of $0.76\text{--}0.25 \text{ h}^{-1}$, molar ratio of methanol-to-oil of $9.16\text{--}13.7$ and temperature of $338\text{--}347 \text{ K}$.

AUTHOR INFORMATION

Corresponding Author

*Tel.: +86-25-52090612. Fax: +86-25-52090612. E-mail: xiaogm@seu.edu.cn.

Notes

The authors declare no competing financial interest.

ACKNOWLEDGMENTS

The authors acknowledged the National High Technology Research and Development Program of China (2009AA03Z222), National Natural Science Foundation of China (21076044 and 20906013), and Major Scientific Research Guiding Program of Southeast University (21076044) for financial support.

NOMENCLATURE

- a = catalyst internal specific surface area ($\text{m}^2 \cdot \text{m}^{-3}$)
- C_{bi0} = initial concentration in bulk fluid of component i ($\text{kmol} \cdot \text{m}^{-3}$)
- C_{bi} = concentration in bulk fluid of component i ($\text{kmol} \cdot \text{m}^{-3}$)
- C_{si} = concentration at the external surface of catalyst of component i ($\text{kmol} \cdot \text{m}^{-3}$)
- D_{eff} = effective diffusivity ($\text{m}^2 \cdot \text{s}^{-1}$)
- D_i = diffusivity of component i ($\text{m}^2 \cdot \text{s}^{-1}$)
- d_p = equivalent diameter of catalyst particle (m)
- d_t = inner diameter of the reactor (m)
- k = rate constant of transesterification reaction ($\text{m}^6 \cdot \text{kmol}^{-1} \cdot \text{kg}^{-1} \cdot \text{s}^{-1}$)
- K = reaction equilibrium constant
- K_i = adsorption equilibrium constant of component i ($\text{m}^3 \cdot \text{kmol}^{-1}$)
- k_{LSi} = mass transfer coefficient at the liquid–solid interface of component i ($\text{m} \cdot \text{s}^{-1}$)
- L = height of catalyst packed in the fixed bed reactor (m)
- LHSV = liquid hourly space velocity (h^{-1})
- m = molar ratio of methanol-to-oil, mole number of methanol: mole number of palm oil
- Δp = pressure drop of fixed bed reactor (Pa)
- p = operation pressure of fixed bed reactor (MPa)
- r = reaction rate excluding mass transfer effects ($\text{kmol} \cdot \text{kg}^{-1} \cdot \text{s}^{-1}$)
- r_e = reaction rate including external diffusion effects ($\text{kmol} \cdot \text{kg}^{-1} \cdot \text{s}^{-1}$)

r_{ei} = reaction rate including both external and internal diffusion effects ($\text{kmol}\cdot\text{kg}^{-1}\cdot\text{s}^{-1}$)
 S_e = catalyst external specific surface area ($\text{m}^2\cdot\text{m}^{-3}$)
 T = absolute temperature (K)
 u_1 = liquid mixture velocity ($\text{m}\cdot\text{s}^{-1}$)
 V_i = molar volume of solute i at normal boiling point ($\text{m}^3\cdot\text{kmol}^{-1}$)
 V_g = catalyst specific pore volume ($\text{m}^3\cdot\text{kg}^{-1}$)
 x = conversion of transesterification reaction

Greek letters

δ = tortuosity factor of catalyst
 ε = void fraction of fixed bed reactor
 η = internal diffusion effectiveness factor
 η_e = external diffusion effectiveness factor
 θ = catalyst porosity
 μ_1 = liquid mixture viscosity ($\text{Pa}\cdot\text{s}$)
 μ_i = viscosity of component i ($\text{Pa}\cdot\text{s}$)
 ξ_B = association factor of solvent B
 ρ_b = packed density of fixed bed reactor ($\text{kg}\cdot\text{m}^{-3}$)
 ρ_i = density of component i ($\text{kg}\cdot\text{m}^{-3}$)
 ρ_1 = liquid mixture density ($\text{kg}\cdot\text{m}^{-3}$)
 ρ_p = catalyst particle density ($\text{kg}\cdot\text{m}^{-3}$)
 ρ_t = catalyst skeletal density ($\text{kg}\cdot\text{m}^{-3}$)
 Φ = Thiele modulus

Abbreviations

1 = subscripted symbol of palm oil
 2 = subscripted symbol of methanol
 3 = subscripted symbol of biodiesel
 4 = subscripted symbol of glycerol

REFERENCES

- (1) Pinzi, S.; Garcia, I. L.; Lopez-Gimenez, F. J.; de Castro, M. D. L.; Dorado, G.; Dorado, M. P. The ideal vegetable oil-based biodiesel composition: A review of social, economical and technical implications. *Energy Fuels* **2009**, *23*, 2325–2341.
- (2) Dalai, A. K.; Kulkarni, M. G. Waste cooking oil-an economical source for biodiesel: A review. *Ind. Eng. Chem. Res.* **2006**, *45* (9), 2901–2913.
- (3) Sivasamy, A.; Cheah, K. Y.; Fornasiero, P.; Kemausor, F.; Zinoviev, S.; Miertus, S. Catalytic applications in the production of biodiesel from vegetable oils. *ChemSusChem* **2009**, *2* (4), 278–300.
- (4) Di Serio, M.; Tesser, R.; Pengmei, L.; Santacesaria, E. Heterogeneous catalysts for biodiesel production. *Energy Fuels* **2008**, *22* (1), 207–217.
- (5) Helwani, Z.; Othman, M. R.; Aziz, N.; Kim, J.; Fernando, W. J. N. Solid heterogeneous catalysts for transesterification of triglycerides with methanol: A review. *Appl. Catal., A* **2009**, *363* (1–2), 1–10.
- (6) Jothiralingam, R.; Wang, M. K. Review of recent developments in solid acid, base, and enzyme catalysts (heterogeneous) for biodiesel production via transesterification. *Ind. Eng. Chem. Res.* **2009**, *48* (13), 6162–6172.
- (7) Ngamprasertsith, S.; Sawangkeaw, R.; Bunyakit, K. A review of laboratory-scale research on lipid conversion to biodiesel with supercritical methanol (2001–2009). *J. Supercrit. Fluids* **2010**, *55* (1), 1–13.
- (8) Tan, K. T.; Lee, K. T. A review on supercritical fluids (SCF) technology in sustainable biodiesel production: Potential and challenges. *Renew. Sustain. Energy Rev.* **2011**, *15* (5), 2452–2456.
- (9) Savage, P. E.; Pinnarat, T. Assessment of noncatalytic biodiesel synthesis using supercritical reaction conditions. *Ind. Eng. Chem. Res.* **2008**, *47* (18), 6801–6808.
- (10) Vu, K. B.; Phan, T. D. N. Biodiesel Production with zinc aluminate catalysts in a high-pressure-fixed-bed-reactor. *Korean Chem. Eng. Res.* **2008**, *46* (1), 189–193.
- (11) McNeff, C. V.; McNeff, L. C.; Yan, B.; Nowlan, D. T.; Rasmussen, M.; Gyberg, A. E.; Krohn, B. J.; Fedie, R. L.; Hoye, T. R. A continuous catalytic system for biodiesel production. *Appl. Catal., A* **2008**, *343* (1–2), 39–48.
- (12) Skala, D.; Glisic, S.; Lukic, I. Biodiesel synthesis at high pressure and temperature: Analysis of energy consumption on industrial scale. *Bioresour. Technol.* **2009**, *100* (24), 6347–6354.
- (13) Chen, J.; Jiang, J. C.; Nie, X. A.; Li, K.; Chang, X.; Wu, H. Kinetics study for continuous transesterification of cottonseed oil in a static mixing tubular reactor to prepare biodiesel. *Linchan Huaxue Yu Gongye* **2011**, *31*, 55–59.
- (14) Ke, Z.; Xi, L.; Yang, W.; Zhu, W. Catalyzed preparation of biodiesel by strong base anion exchange resin in self-made fixed bed reactor. *Zhongguo Liangyou Xuebao* **2011**, *26*, 5.
- (15) Gao, L. J.; Teng, G. Y.; Lv, J. H.; Xiao, G. M. Biodiesel Synthesis Catalyzed by the KF/Ca–Mg–Al Hydrotalcite Base Catalyst. *Energy Fuels* **2010**, *24*, 646–651.
- (16) Chiang, A. S.; Dixon, A. G.; Ma, Y. H. The determination of zeolite crystal diffusivity by gas-chromatography. 2. Experimental. *Chem. Eng. Sci.* **1984**, *39* (10), 1461–1468.
- (17) Perego, C.; Peratello, S. Experimental methods in catalytic kinetics. *Catal. Today* **1999**, *52* (2–3), 133–145.
- (18) Xiao, Y.; Gao, L. J.; Xiao, G. M.; Lv, J. H. Kinetics of the transesterification reaction catalyzed by solid base in a fixed-bed reactor. *Energy Fuels* **2010**, *24*, S829–S833.
- (19) Froment, G. F.; Rijksumiversiteit Gent, B. *Chemical Reactor Analysis and Design*; John Wiley & Sons: New York, 1979; p 178–179.
- (20) Froment, G. F.; Rijksumiversiteit Gent, B. *Chemical Reactor Analysis and Design*; John Wiley & Sons: New York, 1979; p 180–181.
- (21) Froment, G. F.; Rijksumiversiteit Gent, B. *Chemical Reactor Analysis and Design*; John Wiley & Sons: New York, 1979; p 182.
- (22) Satterfield, G. N. *Mass Transfer in Heterogeneous Catalysis*; MIT Press: Cambridge, 1970.
- (23) Anthony, L. H.; Robert, N. M. *Mass Transfer Fundamentals and Applications*; Prentice Hall: Englewood Cliffs, NJ, 1985.
- (24) Baltanas, M. A.; Campanella, A. Degradation of the oxirane ring of epoxidized vegetable oils in liquid–liquid heterogeneous reaction systems. *Chem. Eng. J.* **2006**, *118* (3), 141–152.
- (25) Meng, Z. L.; Jiang, J. C.; Li, X. Y. Co-solvent study and application in biodiesel preparation. *Taiyangneng Xuebao* **2009**, *30*, 385–389.
- (26) Romero, R.; Pena, R.; Martinez, S. L.; Ramos, M. J.; Martinez, A.; Natividad, R. Transesterification of castor oil: Effect of catalyst and co-solvent. *Ind. Eng. Chem. Res.* **2009**, *48* (3), 1186–1189.
- (27) Zhang, L.; Xu, Z. M.; *Chemical Reactor Analysis*; East China University of Science and Technology Press: Shanghai, 2004; p 108.
- (28) Froment, G. F.; Rijksumiversiteit Gent, B. *Chemical Reactor Analysis and Design*; John Wiley & Sons: New York, 1979; p 477.
- (29) Hsieh, L. S.; Kumar, U.; Wu, J. C. S. Continuous production of biodiesel in a packed-bed reactor using shell-core structural $\text{Ca}(\text{C}_3\text{H}_7\text{O}_2)_2/\text{CaCO}_3$ catalyst. *Chem. Eng. J.* **2010**, *158* (2), 250–256.